

State-to-State Quantum Reactive Scattering Calculations and Rate Constant for Nitrogen Atoms in Collision with NO Radicals at Low Temperatures

M. Jorfi and P. Honvault*

Institut UTINAM, UMR CNRS 6213, University of Franche-Comté, 25030 Besançon Cedex, France

Received: July 7, 2009

Total and state-to-state probabilities have been determined for the $\text{N} + \text{NO} \rightarrow \text{N}_2 + \text{O}$ reaction for collision energies up to 0.6 eV using a time-independent quantum mechanical method. The probabilities as a function of collision energy show broad oscillations, in strong contrast with previous theoretical results obtained by means of a time-dependent wave packet method that show a dense resonance structure. The rate constant has been calculated in the J-shifting approach for temperatures between 10 and 400 K. It is in good agreement with previous theoretical results obtained only at 100 K and above 200 K and experiments in a wide temperature range.

Introduction

The exothermic $\text{N}(^4\text{S}) + \text{NO}(X^2\Pi) \rightarrow \text{N}_2(X^1\Sigma_g^+) + \text{O}(^3\text{P})$ ($\Delta H_0^\circ = -3.25$ eV) reaction is involved in the chemistry of NO and N_2 in the interstellar medium and in planetary atmospheres.¹ If we accept the current models of interstellar clouds, the major source of nitric oxide is the $\text{N} + \text{OH} \rightarrow \text{NO} + \text{H}$ reaction, whereas the main destruction reaction is $\text{N} + \text{NO} \rightarrow \text{N}_2 + \text{O}$. The present study is motivated by the need to get a more accurate value of the rate constant for $\text{N} + \text{NO}$ employed in the astrochemical models. Recommended values given by the databases^{2–4} currently use at low temperatures extrapolated values. The very recent new measurements of Bergeat et al.¹ of the rate constant for the $\text{N} + \text{NO} \rightarrow \text{N}_2 + \text{O}$ reaction at low temperatures ($48 \text{ K} < T < 211 \text{ K}$) have also initiated the present work. It is interesting to note that the lowest temperature in this experiment is not low enough for the production of N_2 in the cold, dense interstellar clouds where the typical temperature is 10 K. Many other experimental measurements of the rate constant have been carried out before, but they are restricted to measurements at room temperature for most of them (see ref 1 and references therein). On the theoretical side, atomic nitrogen in its ground state with the ground $^2\Pi$ state of NO leads to four potential energy surfaces (PESs), but only two, $^3\text{A}''$ and $^3\text{A}'$, give $\text{N}_2(X^1\Sigma_g^+) + \text{O}(^3\text{P})$.^{5,6} The ground $^3\text{A}''$ PES is barrierless for $\text{N} + \text{NO} \rightarrow \text{N}_2 + \text{O}$, whereas the $^3\text{A}'$ PES has a barrier of 0.38 eV (including the zero-point energy). Quasiclassical trajectory (QCT) and reduced quantum approaches⁷ have employed an analytical PES based on limited ab initio information⁵ for the ground $^3\text{A}''$ state. Other QCT calculations have been performed^{8,9} on a semiempirical London–Eyring–Polanyi–Sato surface. Recently, Gamallo et al.¹⁰ have built new analytical fits of the $^3\text{A}''$ and $^3\text{A}'$ states based on high-level ab initio calculations.⁶ Then, time-dependent wave packet (TDWP) calculations were carried out¹¹ on the ground PES using the J-shifting approximation, giving a rate constant for temperatures between 100 and 2000 K. More recent TDWP calculations¹² on both the ground and excited PESs have yielded a rate constant between 200 and 2500 K that agrees well with experimental results. However, no theoretical data are given for temperatures lower than 100 K. At low energies, the TDWP cross section

obtained on the ground PES decreases,^{11,12} in contrast with the barrierless nature of the reaction. It is well-known that the wave packet methods have difficulty in accurately describing dynamics at low temperature (see, for instance, the TDWP results for the barrierless $\text{O} + \text{OH}$ reaction¹³). As a result, a characterization of the reaction dynamics at low temperatures using an accurate time-independent quantum mechanical (TIQM) method that avoids these drawbacks is highly desirable. In the present work, we have carried out a study of the $\text{N} + \text{NO} \rightarrow \text{N}_2 + \text{O}$ reaction dynamics by means of a TIQM approach. Total and state-to-state reaction probabilities have been computed at a total angular momentum $J = 0$ for collision energies up to 0.6 eV. Using the J-shifting method,¹⁴ we obtain the rate constant in the 10–400 K temperature range. To the best of our knowledge, calculations of the rate constant at the lowest temperatures ($T < 100 \text{ K}$) have not yet been investigated by a quantum method, and a comparison between quantum mechanical (QM) results and experiment below 200 K has not yet been reported.

Quantum Mechanical Method

All the QM scattering calculations presented here have been performed for $\text{N} + \text{NO} (v = 0, j = 0) \rightarrow \text{N}_2(v', j') + \text{O}$ on the $^3\text{A}''$ ground PES.¹⁰ We have used a TIQM based on body-frame democratic hyperspherical coordinates. Details of the hyperspherical method can be found in ref 15. This method has also previously proved successful in describing the quantum dynamics of atom–diatom insertion reactions, such as $\text{N}(^2\text{D}) + \text{H}_2 \rightarrow \text{NH} + \text{H}$;¹⁶ ultracold alkali–diatomic collisions;¹⁷ and, more recently, OH + atom reactions.^{18,19} The crucial parameters for obtaining convergence in the hyperspherical method are essentially the number of states to include and the asymptotic matching distance. It is essential to include many closed channels. For the $J = 0$ partial wave, the scattering wave function was expanded on the basis of 900 states, and the matching distance was chosen as $10.1a_0$. The system $\text{N} + \text{NO}$ is very difficult and demanding among the atom + diatom reactions because all three atoms are heavy and the exoergicity is large. However, the permutation symmetry allows such QM calculations, as for $\text{O} + \text{OH}$.¹⁸ In addition, as in all recent investigations of reactions involving the $X^2\Pi$ state of OH, such as $\text{N} + \text{OH}$ ^{19,20} or $\text{O} + \text{OH}$ (see ref 21 and references therein), we ignored in this study the electronic orbital and spin angular

* Corresponding author. E-mail: pascal.honvault@univ-fcomte.fr.

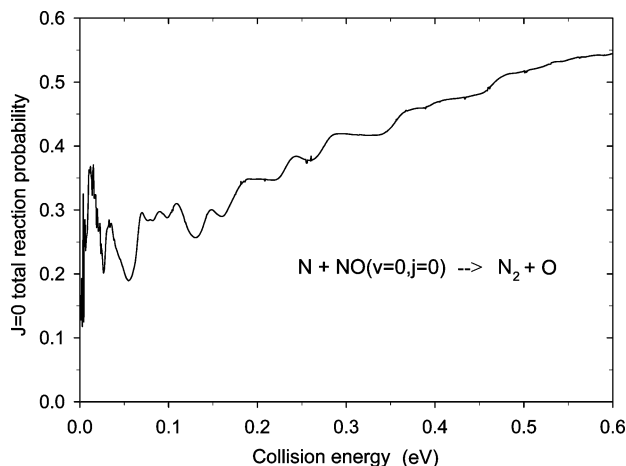


Figure 1. Total reaction probability as a function of collision energy for the $\text{N} + \text{NO}(v=0, j=0) \rightarrow \text{N}_2 + \text{O}$ reaction.

momenta, assuming that the rotational level structure of the reactant NO diatomics was that of a closed-shell molecule. So in this first QM study of $\text{N} + \text{NO}$ at $J=0$ by our group, we consider only the reactants NO in their lowest rovibrational state ($v=0, j=0$).

Results and Discussion

We computed total and state-to-state reaction probabilities for the $\text{N} + \text{NO}(v=0, j=0) \rightarrow \text{N}_2(v', j') + \text{O}$ reaction at $J=0$. Calculations have been performed in the 0–0.6 eV collision energy range on a regular grid with a step of 0.0005 eV. Finally, as mentioned in refs 11 and 12, the N_2 permutation and nuclear-spin symmetries have been taken into account in the present work. So the rotational states j' of N_2 in its ground electronic state $^1\Sigma_g^+$ have the statistical weights equal to 2/3 and 1/3 for even and odd j' , respectively.

Figure 1 shows the total reaction probability as a function of collision energy. The absence of barrier in the PES for the $\text{N} + \text{NO}$ entrance arrangement leads to a total reaction probability which has no energy threshold. Due to the opening of more and more rovibrational states of N_2 , the average probability globally increases as the collision energy increases. It is in good agreement with the average of the TDWP reaction probability of Gamallo et al.¹¹ for $\text{NO}(v=0, j=0)$ on the same PES. It is also interesting to note that the reactivity is not unity, indicating significant backscattering, despite the fact that there is no barrier along the minimum energy path for the $\text{N} + \text{NO} \rightarrow \text{N}_2 + \text{O}$ reaction. The curve in Figure 1 has some broad oscillations that disappear at high collision energy. The TIQM reaction probability does not thus show any sharp peak structure, in strong contrast with the TDWP results of Gamallo et al.^{11,12} which give an extremely dense resonant structure in the 0–1 eV collision energy range.

QM resonances in neutral–neutral reactions are usually associated with a deep well (typically several electron-volts) that supports a large number of bound states and gives rise to the formation of a long-lived intermediate complex with a lifetime that can be longer than its rotational period. However, the resonance peaks are very intense and sharp if the exoergicity is small. In contrast, higher exoergic reactions yield a faster decay and broader resonance widths. For instance, in the exothermic $\text{C}(^1\text{D}) + \text{H}_2 \rightarrow \text{CH} + \text{H}$ reaction characterized by a deep well (4.29 eV relative to the entrance channel) and an exoergicity of 0.26 eV only, a dense resonance structure was found, and the average lifetime of the resonant states of CH_2

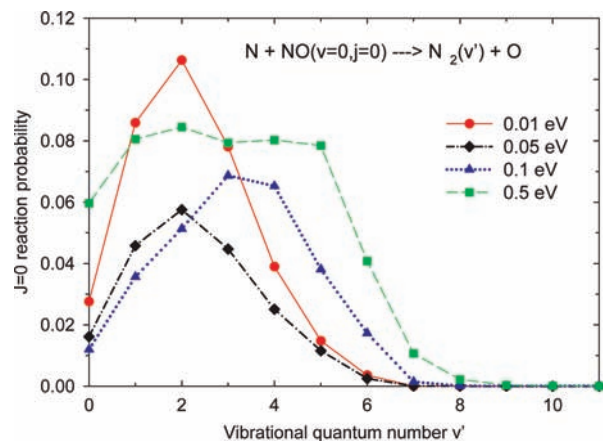


Figure 2. Product vibrational distributions at $J=0$: vibrational state resolved reaction probabilities as a function of vibrational quantum number v' of N_2 at 0.01 (solid line), 0.05 (dashed–dotted line), 0.1 (dotted line), and 0.5 eV (dashed line).

has been estimated around 1 ps.²² This is in strong contrast with the $\text{O}(^1\text{D}) + \text{H}_2 \rightarrow \text{OH} + \text{H}$ reaction, which involves a deeper well (7.29 eV) but a much larger exoergicity (1.92 eV), yielding reaction probabilities with large undulations.²³ Similar trends have been found for the exothermic $\text{C} + \text{NO} \rightarrow \text{CN} + \text{O}$ reaction,²⁴ which involves a deep well of 4.20 eV and an exoergicity of 1.35 eV. The numerous and sharp resonances found using our TIQM method in $\text{C}(^1\text{D}) + \text{H}_2$ ²² reaction have also been found using a TDWP quantum method.²⁵ Comparison between the results obtained by the two methods shows excellent agreement, but two light atoms were involved in these reactions. The very small exoergicity of barrierless reactions involving a deep well thus appears as an essential feature to obtain narrow resonances.²³

The present TIQM results on $\text{N} + \text{NO} \rightarrow \text{N}_2 + \text{O}$ are consistent with the features of this reaction: no well in the PES between the reactants and products,^{6,10} mechanism of direct abstraction type,^{12,11} and large exoergicity. A direct mechanism has been suggested, for instance, by QCT calculations⁷ on an earlier PES⁷ which gave differential cross sections with a predominant backward scattering. An inverted product vibrational distribution has been found by the same QCT calculations as well as by recent TDWP calculations¹² on the PES used in the present work and by other QCT calculations⁹ using another PES.⁸ These two features are usually observed for a direct reaction involving a short-lived intermediate complex. Vibrational distributions (reaction probability as a function of the N_2 quantum vibrational number v') at $J=0$ are plotted in Figure 2 at four collision energies: 0.01, 0.05, 0.1, and 0.5 eV. The lowest vibrational state, $v'=0$, is not favored, and the distributions appear inverted at all collision energies. This behavior is consistent with a reaction mainly dominated by a direct mechanism.

We find that even at the state-to-state level, no resonances are found. For instance, in Figure 3, the state-to-state reaction probabilities for $\text{N} + \text{NO}(v=0, j=0) \rightarrow \text{N}_2(v'=0, j=40, 41) + \text{O}$ are plotted as a function of collision energy. The structure is more marked than in the total reaction probability, but the oscillations remain broad. We also find that the rotationally state-resolved reaction probabilities depend strongly on the final rotational state j' of N_2 (results not shown here). Figure 3 shows that the probabilities for the $j'=40, 41$ states are much larger at low energy (below 0.1 eV) and at high energy (above 0.5 eV) than at medium energy, showing a strong effect

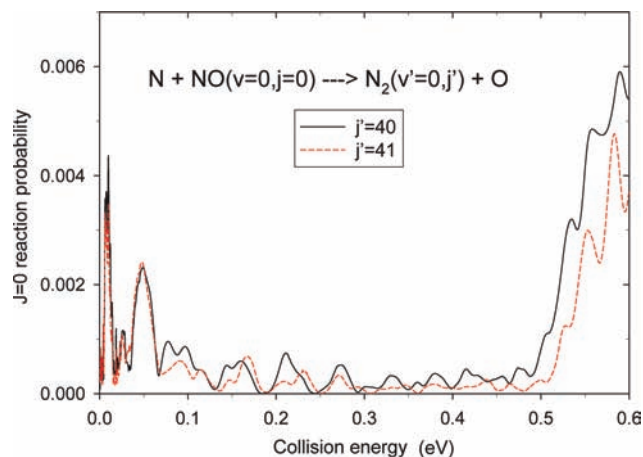


Figure 3. Rotationally state-resolved probabilities as a function of collision energy for the $\text{N} + \text{NO}(v=0, j=0) \rightarrow \text{N}_2(v'=0, j'=40, 41) + \text{O}$ reaction.

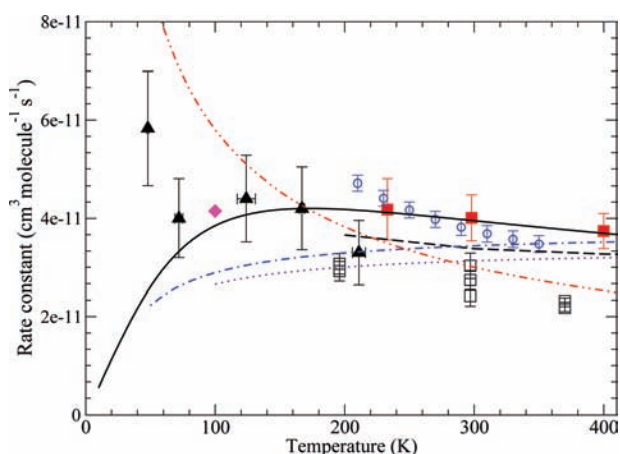


Figure 4. Theoretical and experimental rate constants for the $\text{N} + \text{NO} \rightarrow \text{N}_2 + \text{O}$ reaction. Solid line, this work; dashed line, TDWP calculations of Gamallo et al.;¹² diamond at 100 K, TDWP calculation of Gamallo et al.;¹¹ dotted line, QCT calculations of Duff and Sharma;⁸ solid triangles, measurements of Bergeat et al.;¹ solid squares (FP–RF) and open squares (DF–RF), measurements of Lee et al.;²⁸ open circles, measurements of Wennberg et al.;²⁹ dashed–dotted line, UMIST06;³ and dashed–dotted–dotted line, OSU2008.⁴

of the collision energy on the reactivity. At some collision energies, the reaction probability is even very small, reaching zero for a few collision energies.

The rate constant is obtained using the exact TIQM reaction probability for $J = 0$ and the reaction probabilities for $J > 0$ calculated in the J-shifting approach.¹⁴ We have already used this procedure in the barrierless $\text{O} + \text{OH}$ reaction.^{18,26} To compare the theoretical rate constant to the rate measured in experiments, we have multiplied it by a temperature-dependent electronic factor²⁷ to take into account the fine structure distribution of $\text{NO}(X^2\Pi)$ and the degeneracies of the electronic states of NNO and $\text{N}(^4\text{S})$. The excited vibrational states of NO , $v > 0$, have not been considered in this study because only the ground vibrational state, $v = 0$, contributes to the rate constant below 400 K. The rate constant as a function of temperature is displayed in Figure 4 and compared with the most recent measurements,¹ previous experimental data,^{28,29} theoretical results,^{8,11,12} and rate constants found in the astrochemical databases (UMIST06³ and OSU2008⁴). Our results are in good agreement, even quantitatively, with the measurements of Bergeat et al.¹ if we restrict the comparison with the measurements to the three experimental points obtained at 72, 124, and

167 K. Our prediction underestimates the experimental data at 48 K while it slightly overestimates the measurement at 211 K. The TIQM results are in excellent agreement with the experiments of Lee et al.²⁸ for the measurements using the flash photolysis–resonance fluorescence (FP–RF) technique, but they overestimate the measurements by the same group²⁸ using the discharge flow–resonance fluorescence (DF–RF) technique. Finally, the TIQM rate constant is in fairly good agreement with the experimental data of Wennberg et al.²⁹

Interestingly, the TDWP values of the rate constant obtained from the most recent calculations of Gamallo et al.¹² slightly underestimate the TIQM values in the 200–400 K temperature range. Moreover, their result at 100 K from an earlier TDWP calculation¹¹ is close to the TIQM result. Given the large differences found between the TIQM and TDWP reaction probabilities as mentioned above, this is a somewhat surprising outcome. In fact, the average reaction probabilities are nearly identical and then may yield similarities between the two rate constants. However, if we also consider the TDWP point at 100 K, the temperature dependence of the rate constant for $100 \text{ K} < T < 400 \text{ K}$ is not the same for the two calculations, with opposite curvatures. Since only the lowest internal state of NO was considered in the TIQM calculation, overestimation of the TIQM rate constant in the 200–400 K temperature range may be attributed to the neglect of rotationally excited NO . Indeed, in some cases, such as the $\text{N} + \text{OH}$ reaction,^{20,30} the rotational excited states of reactants yield smaller specific rate constants than the ground rovibrational state rate constant at low temperature. Then the thermal rate constant is below the rate constant calculated without initial rotational excitation.

The TIQM rate constant is much larger than the QCT rate constant of Duff and Sharma⁸ for temperatures above 100 K. This disagreement may be linked to the QCT method, which is based on classical mechanics, so the zero-point energy is not rigorously accounted and quantum effects cannot occur. Finally, the present result is in total disagreement below 100 K for both magnitude and temperature dependence with the OSU2008 rate constant, whereas it is closer to the UMIST06 rate constant with respect to the temperature dependence. The values of the rate constant computed in the present work for temperatures between 10 and 400 K with a step of 1 K are available upon request from the authors of this article.

Conclusions

In this article, we report total and state-to-state reaction probabilities of the $\text{N} + \text{NO}(v=0, j=0) \rightarrow \text{N}_2(v', j') + \text{O}$ reaction for $J = 0$ in the 0–0.6 eV collision energy range calculated on the ground-state PES by means of an accurate TIQM method. The total reaction probability has been compared with the reaction probability obtained using a TDWP approach^{11,12} on the same PES from 0 to 0.6 eV. Although the TIQM and TDWP reaction probabilities are found to have a similar increase with the collision energy, the highly oscillatory structure present in the TDWP calculation, due apparently to quantum resonances, is not present in the TIQM prediction. Such a dense resonance structure is also absent in the state-to-state TIQM reaction probabilities. The rate constant was then obtained using the exact $J = 0$ reaction probability and a J-shifting method for $J > 0$ in the 10–400 K temperature range. It is in good agreement with the most recent measurements at low temperature (with the exception at the lowest temperature, 48 K) and with previous available experimental data. The new findings reported here suggest that our current understanding of this important reaction need more accurate QM calculations and experimental results,

especially at low temperatures of atmospheric and astrophysical interest. A first necessary improvement is the removal of the J-shifting approximation. Other product state-resolved information, such as the state-to-state differential sections, are desirable. To this goal, it is necessary to use a TIQM method without dynamic approximations whose main advantage over the wave packet approach is the accurate determination of scattering attributes at low energies and temperatures. Work in these directions is underway in our group.

Acknowledgment. We thank A. Bergeat for providing us their experimental data before publication and for helpful discussions. We acknowledge computational support from the Pole de Sciences Planétaires Bourgogne Franche-Comté as well as from the Programme National Physique Chimie du Milieu Interstellaire.

References and Notes

- (1) Bergeat, A.; Hickson, K. M.; Daugey, N.; Caubet, P.; Costes, M. *Phys. Chem. Chem. Phys.*, in press.
- (2) Sander, S. P., et al. *Chemical Kinetics and Photochemical Data for Use in Atmospheric Studies Evaluation, Number 15*; NASA Jet Propulsion Laboratory (JPL): Pasadena, CA, 2006.
- (3) Woodall, J.; Agundez, M.; Markwick-Kemper, A. J.; Millar, T. J. *Astron. Astrophys.* **2007**, *466*, 1197.
- (4) Herbst, E. OSU 09-2008 Database **2008**; <http://www.physics.ohio-state.edu/~eric/research.html>.
- (5) Walch, S. P.; Jaffe, R. L. *J. Chem. Phys.* **1987**, *86*, 6946.
- (6) Gamallo, P.; González, M.; Sayós, R. *J. Chem. Phys.* **2003**, *118*, 10602.
- (7) Gilibert, M.; Aguilar, A.; González, M.; Mota, F.; Sayós, R. *J. Chem. Phys.* **1992**, *97*, 5542. Gilibert, M.; Aguilar, A.; González, M.; Sayós, R. *J. Chem. Phys.* **1993**, *99*, 1719. Aguilar, A.; Gilibert, M.; Gimenez, X.; González, M.; Sayós, R. *J. Chem. Phys.* **1995**, *103*, 4496.
- (8) Duff, J. W.; Sharma, R. D. *Geophys. Res. Lett.* **1996**, *23*, 2777.
- (9) Duff, J. W.; Sharma, R. D. *Chem. Phys. Lett.* **1997**, *265*, 404.
- (10) Gamallo, P.; González, M.; Sayós, R. *J. Chem. Phys.* **2003**, *119*, 2545.
- (11) Gamallo, P.; González, M.; Sayós, R.; Petrongolo, C. *J. Chem. Phys.* **2003**, *119*, 7156.
- (12) Gamallo, P.; Sayós, R.; González, M.; Petrongolo, C.; Defazio, P. *J. Chem. Phys.* **2006**, *124*, 174303.
- (13) Jorfi, M.; Honvault, P.; Halvick, P.; Lin, S. Y.; Guo, H. *Chem. Phys. Lett.* **2008**, *462*, 53.
- (14) Bowman, J. M. *J. Phys. Chem.* **1991**, *95*, 4960.
- (15) Honvault, P.; Launay, J.-M. *Theory of Chemical Reaction Dynamics*; Lagana, A., Lendvay, G., Eds.; Kluwer: Dordrecht, The Netherlands, 2004; p 187.
- (16) Balucani, N.; Cartechini, L.; Capozza, G.; Segoloni, E.; Casavecchia, P.; Volpi, G. G.; Aoiz, F. J.; Banares, L.; Honvault, P.; Launay, J.-M. *Phys. Rev. Lett.* **2002**, *89*, 013201.
- (17) Cvitas, M. T.; Soldan, P.; Hutson, J. M.; Honvault, P.; Launay, J. M. *Phys. Rev. Lett.* **2005**, *94*, 033201.
- (18) Xu, C.; Xie, D.; Honvault, P.; Lin, S. Y.; Guo, H. *J. Chem. Phys.* **2007**, *127*, 024304.
- (19) Jorfi, M.; Honvault, P. *J. Phys. Chem. A* **2009**, *113*, 2316.
- (20) Edvardsson, D.; Williams, C. F.; Clary, D. C. *Chem. Phys. Lett.* **2006**, *431*, 261.
- (21) Jorfi, M.; Honvault, P.; Bargueno, P.; González-Lezana, T.; Larrégaray, P.; Bonnet, L.; Halvick, P. *J. Chem. Phys.* **2009**, *130*, 184301.
- (22) Bussery-Honvault, B.; Honvault, P.; Launay, J.-M. *J. Chem. Phys.* **2001**, *115*, 10701.
- (23) Rackham, E. J.; González-Lezana, T.; Manolopoulos, D. E. *J. Chem. Phys.* **2003**, *119*, 12895.
- (24) Monnerville, M.; Péoux, G.; Briquez, S.; Halvick, P. *Chem. Phys. Lett.* **2000**, *322*, 157.
- (25) Mouret, L.; Launay, J.-M.; Terao-Dunseath, M.; Dunseath, K. *Phys. Chem. Chem. Phys.* **2004**, *6*, 4105.
- (26) Lique, F.; Jorfi, M.; Honvault, P.; Halvick, P.; Lin, S. Y.; Guo, H.; Xie, D.; Klos, J.; Dagdigian, P. J.; Alexander, M. H. submitted.
- (27) Graff, M. M.; Wagner, A. F. *J. Chem. Phys.* **1990**, *92*, 2423.
- (28) Lee, J. H.; Michael, J. V.; Payne, W. A.; Stief, L. J. *J. Chem. Phys.* **1978**, *69*, 3069.
- (29) Wennberg, P. O.; Anderson, J. G.; Weisenstein, D. K. *J. Geophys. Res.* **1994**, *99*, 18839.
- (30) Jorfi, M.; Honvault, P.; Halvick, P. *Chem. Phys. Lett.* **2009**, *471*, 65.

JP907865A